

# Intermittency from Instanton Calculus at the Transition to Turbulence and Fusion Rules

Timo Schorlepp<sup>1,\*</sup> and Rainer Grauer<sup>2,†</sup>

<sup>1</sup>*Courant Institute of Mathematical Sciences, New York University, New York, NY, USA*

<sup>2</sup>*Institute for Theoretical Physics I, Ruhr University Bochum, Bochum, Germany*

(Dated: December 4, 2025)

Understanding intermittency of turbulent systems from the underlying differential equations is an outstanding problem in fluid dynamics. Here, in the example of Burgers turbulence, we introduce a method that yields structure function exponents by combining instanton calculus and fusion rule predictions. We use instantons to evaluate velocity gradient (VG) moments at the onset of intermittency, and then infer scaling exponents in fully developed turbulence via fusion rules. We show that the method captures the phase transition at  $\text{Re}_\lambda \approx 1$  in the VG moment scaling, highlight the necessity of including fluctuations around instantons, and discuss future extensions.

*Introduction.* Turbulence is often referred to as the last unsolved problem in classical physics [1]. Of outstanding importance is the understanding of the anomalous scaling of structure functions or, equivalently, of the non-self-similar behavior of probability distribution functions (PDFs) of velocity increments, leading from nearly Gaussian shapes at large separations of the increments to distributions with heavy tails at small distances [2]. Various theoretical methods have been used so far to tackle this problem. One class of methods is represented by phenomenological models [3–10], which use only global properties of the underlying partial differential equations (PDEs) such as the Navier–Stokes equations (NSE), Burgers equation, magnetohydrodynamic equations, e.g. about a direct energy cascade due to a quadratic nonlinearity of advection type, or about properties of dissipation at localized structures. These models have shown remarkable agreement with experiments or direct numerical simulations (DNS), and have highlighted the importance of accounting for quasi-singularities such as vortex tubes, sheets or shocks [11]. However, phenomenological models usually have free parameters that are not determined from the underlying PDE, and the geometry of quasi-singular structure is inferred from experiments or numerical simulations. Another class of methods follows a direct way, i.e., to determine from the underlying PDE the properties of the energy spectrum, structure functions and increment statistics. These methods are extremely diverse and mostly motivated from quantum and statistical field theory. A distinction can be made between perturbative (direct interaction approximation [12, 13], renormalization group [14, 15]) and non-perturbative methods (fusion rules [16–18], replica symmetry breaking [19], functional renormalization group [20–22], instanton calculus [23–30]). We also mention the access to vorticity statistics via area laws [31–33] and the detailed numerical studies of fusion rules [34, 35].

*Our approach.* We present a theoretical, non-perturbative method in this Letter which computes struc-

ture function exponents at large Reynolds numbers ( $\text{Re}$ ) by combining the instanton approach for velocity gradient (VG) moments at low to moderate  $\text{Re}$  with results from fusion rules. This is conceptually in line with recent works [36–38] which use VG information at the onset of intermittency to draw conclusions about flows at asymptotically large  $\text{Re}$ . We emphasize that while the presented approach requires considerable technical effort, and we rely on numerical computations to evaluate the instanton predictions, it provides a physically interpretable and justifiable route towards understanding turbulence. We demonstrate the method on the example of Burgers turbulence [39–41]. This is a difficult problem since intermittency is particularly strong and the distributions of velocity increments and VGs strongly deviate from Gaussianity. In another sense, however, Burgers turbulence is simple, since the dominant structures, shocks, are extremely stable and do not allow for symmetry breaking as, e.g., the transition from vortices to sheets in the NSE [42], which would require the inclusion of zero modes [30, 43] in our approach. Hence, Burgers turbulence forms an ideal test bed for the method.

*Outline.* We first recall the path integral formulation of Burgers turbulence, which is the basis for approximating statistical quantities using instantons and fluctuations around them [44]. We then briefly introduce fusion rules for moments of VGs in Burgers turbulence [34], and present the  $\text{Re}$  dependence of the normalized VG moments

$$M_n = \frac{\langle (\partial_x u)^n \rangle}{\langle (\partial_x u)^2 \rangle^{n/2}}, \quad (1)$$

and their relation to structure function exponents  $\zeta_q$ . Using instantons and Gaussian fluctuations around them, the normalized VG moments are calculated accurately at moderate  $\text{Re}$  as shown in Fig. 1, and combining this with fusion rules, the anomalous exponents of structure functions at large  $\text{Re}$  are computed. In the conclusion, we critically summarize our results and give an outlook on open questions, further improvements and the appli-

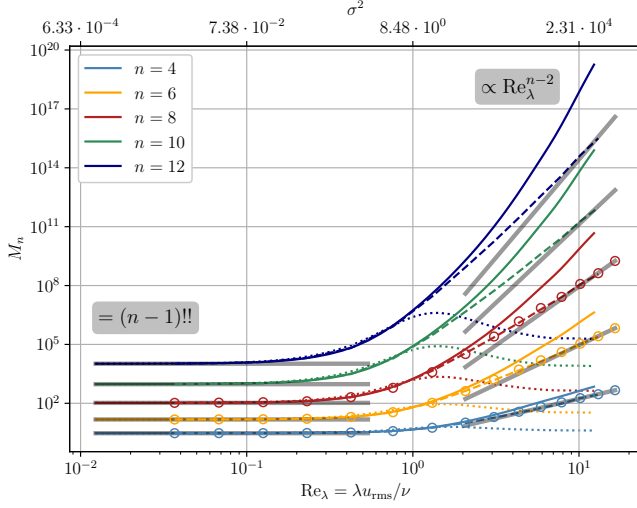


FIG. 1. Normalized VG moments  $M_n$  (Eq. (1)) at different Taylor-Reynolds numbers  $Re_\lambda$  from integrating (i) only the instanton contribution  $\rho(a) \approx \text{const} \times \exp(-S^I(a)/\sigma^2)$  to the VG PDF (dotted lines), (ii) the one-loop approximation (4) including Gaussian fluctuations around the instanton (solid lines), and (iii) Eq. (4) for the  $n$ -th moment in the numerator of Eq. (1) with rescaled left PDF tail, and DNS for the second moment in the denominator of Eq. (1) (dashed lines). Open circles show the results from DNS of Eq. (2). The gray lines indicate the theoretically expected behavior.

cation of the method to other turbulent systems, such as incompressible 3D NSE turbulence.

*Burgers turbulence and instantons.* Consider the stochastic Burgers equation

$$\partial_t u + u \partial_x u - \partial_{xx} u = \chi^{1/2} * \eta, \quad (2)$$

with periodic boundary conditions in space, and Gaussian forcing

$$\langle \eta(x, t) \eta(x', t') \rangle = \sigma^2 \delta(x - x') \delta(t - t'), \quad (3)$$

acting only on large length scales through  $\chi$ . For concreteness, we consider  $\chi(x) = -\partial_{xx}(e^{-x^2/2})$ , in a box of size  $L_{\text{box}} = 2\pi$ . In the units of Eq. (2) with viscosity  $\nu = 1$ , the Reynolds number  $Re$  is varied through the forcing variance  $\sigma^2$ . All quantities that we are interested in can be written as  $\langle f[u(\cdot, T)] \rangle$  where the average is with respect to the forcing, and  $T = 1$  large enough that the system is approximately statistically stationary.

The instanton approach is based on a saddle point approximation of the Martin-Siggia-Rose-Janssen-de Dominicis path integral formulation [45–47] for averages over Eq. (2). The method consists of three steps [27]: (i) calculation of the instanton configuration, the extremum; (ii) calculation of the contributions from fluctuations around the instanton, a functional determinant at leading order; (iii) contributions of broken continuous symmetries through zero modes, if necessary [30, 43].

In this work, we compute the one-point PDF of the VG  $\rho(a) = \langle \delta(\partial_x u(0, T) - a) \rangle$  this way at moderate  $Re$  or  $\sigma^2$ , and combine the results with fusion rules introduced below. The instanton approximation to the PDF is exact in the limit  $\sigma^2 \rightarrow 0$ , when the flow is Gaussian, but also in the limit  $|a| \rightarrow \infty$  at fixed  $\sigma^2$ , i.e. for high moments of the VG  $\langle \partial_x u^n \rangle$  with  $n \gg 1$  which depend on the tails of the gradient PDF. In particular, while the computation of instantons for the Burgers equation is well-established [48–50], a series of recent works [43, 51–55] has made it possible to evaluate the contribution of Gaussian fluctuations around the instanton in closed form. This step considerably improves the accuracy of the instanton approximation. We follow the Fredholm determinant approach of Refs. [53, 55] to compute the fluctuations.

For a range of VG values  $a$ , we approximate the VG PDF to one-loop order around the instanton via

$$\rho(a) \approx (2\pi\sigma^2)^{-1/2} C(a) e^{-S^I(a)/\sigma^2} \quad (4)$$

by (i) numerically finding the instanton field  $u_a^I(x, t)$  that globally minimizes the action [56, 57]

$$S[u] = \frac{1}{2} \int_0^T dt \int_0^{L_{\text{box}}} dx [\partial_t u + u \partial_x u - \partial_{xx} u] \chi^{-1} * [\dots]$$

(where  $[\dots]$  stands for a repetition of the previous term) under the constraints  $u(x, 0) = 0$  and  $\partial_x u(0, T) = a$ . For the present problem, there is a unique instanton  $u_a^I$  for each  $a$ , and we write  $S^I(a) = S[u_a^I]$  for its action, yielding the exponential contribution in Eq. (4). The instanton  $u = u_a^I$ , with conjugate momentum density  $p = p_a^I$  and Lagrange multiplier  $\mathcal{F}_a$ , satisfies the instanton equations [23, 25, 48]

$$\begin{cases} \partial_t u + u \partial_x u - \partial_{xx} u = \chi * p, \\ \partial_t p + u \partial_x p + \partial_{xx} p = 0, \\ u(x, 0) = 0, \quad \partial_x u(0, T) = a, \\ p(x, T) = -\mathcal{F}_a \delta'(x), \end{cases} \quad (5)$$

Our numerical, optimal control-based approach to solve this problem follows Ref. [42]. (ii) The prefactor  $C(a)$ , in a Gaussian approximation of fluctuations around the instanton, is given by [53, 55]

$$C(a) = |\mathcal{F}_a| / (2S^I(a) \det(\text{Id} - B_a))^{1/2}. \quad (6)$$

Here,  $\det$  is a Fredholm determinant which can be computed iteratively [58], in a matrix-free way, by finding the largest eigenvalues of the integral operator  $B_a$ . For this, we only need to apply the second variation operator  $B_a$  to different test noise perturbations  $\delta\eta(x, t)$ : We have  $B_a \delta\eta = \mathcal{P}[\chi^{1/2} * \delta p]$  where  $\delta p$  is found through

solving [53, 55]

$$\begin{cases} \partial_t \delta u + \partial_x (u_a^I \delta u) - \partial_{xx} \delta u = \chi^{1/2} * \mathcal{P}[\delta \eta], \\ \partial_t \delta p + u_a^I \partial_x \delta p + \delta u \partial_x p_a^I + \partial_{xx} \delta p = 0, \\ \delta u(x, 0) = 0, \\ \delta p(x, T) = 0, \end{cases} \quad (7)$$

with  $\mathcal{P}$  the  $L^2$ -orthogonal projection onto  $(\chi^{1/2} * p_a^I)^\perp$ . As in Ref. [44], we use a pseudo-spectral spatial discretization of all equations with resolutions  $n_x \in \{512, 2048\}$ , as well as the Heun scheme with integrating factor for the time stepping with  $n_t = 10^4$  equidistant time steps for the instanton computations. Instantons and prefactors were computed for approximately 500 values of  $a \in [-30000, -0.1]$  and 70 values of  $a \in [0.1, 223]$  (since the positive tail is strongly suppressed), both logarithmically spaced, with 200 dominant eigenvalues of  $B_a$  per  $a$  to approximate the Fredholm determinant (6). This computation needs to be done only once and can then be rescaled to different  $\sigma^2$  and hence  $\text{Re}$  via Eq. (4).

In addition to the instanton computations, we also perform  $10^4$  independent DNS runs of Eq. (2) until  $T = 1$  for different forcing variances  $\sigma^2 \in [10^{-2}, 3 \cdot 10^5]$  with  $n_x = 2048$ , both to have data to compare our instanton predictions to, as well as to obtain the Taylor–Reynolds number  $\text{Re}_\lambda = \lambda u_{\text{rms}}/\nu$  (where  $\nu = 1$ ,  $u_{\text{rms}} = \sqrt{\langle u^2 \rangle}$ , and  $\lambda = u_{\text{rms}} \sqrt{2\nu/\langle \varepsilon \rangle}$  with  $\varepsilon = 2\nu (\partial_x u)^2$ ) as a function of  $\sigma^2$ , as shown in Fig. 4. For small  $\sigma^2$ , when the flow is approximately Gaussian, we have  $\text{Re}_\lambda \propto \sigma$ , and for large  $\sigma^2$  this becomes  $\text{Re}_\lambda \propto \text{Re}^{1/2} \propto \sigma^{1/3}$  [42, 49, 51].

*Fusion rules.* Fusion rules [16–18] relate scaling laws of fused observables, such as gradients, to the  $\text{Re}$  scaling of multi-point observables as those points collapse. Here, since the Burgers Eq. (2) is pressure-less, we apply the fusion rules of Ref. [17]. We consider the standardized even-order VG moments given by Eq. (1). At low  $\text{Re}$ , the one-point statistics of  $u$  and its derivatives are Gaussian, hence we have constant  $M_n(\text{Re}_\lambda \ll 1) \approx (n-1)!!$ . At  $\text{Re}_\lambda \approx 1$ , there is a transition to turbulence, with the theoretical result [34]

$$M_n(\text{Re}_\lambda \gg 1) \propto \text{Re}_\lambda^{n-2} \quad (8)$$

at large  $\text{Re}$ . Remarkably, the standardized VG moments were shown to display this scaling already at moderate  $\text{Re}_\lambda \gtrsim 1$  in DNS [34]. The exponents  $\zeta_q$  of structure functions

$$S_q(r) = \langle |u(x+r) - u(x)|^q \rangle \propto r^{\zeta_q} \quad (9)$$

for  $r$  in the inertial range at large  $\text{Re}$  are well-known:

$$\zeta_q = \min\{1, q\} \quad (10)$$

for the Burgers Eq. (2). In general, the fusion rules derived in Ref. [17] (see also Ref. [34]), adapted to the case considered here, imply

$$M_n(\text{Re}_\lambda \gg 1) \propto \text{Re}_\lambda^{\theta_n}, \quad (11)$$

TABLE I. Scaling exponents  $\theta_n$  of the normalized VG moments (1), as determined from Fig. 1 (dashed lines).

$n$	$\theta_n$ (computed)	$\theta_n$ (theory)	rel. error (%)
4	1.83	2	−8.6
6	3.47	4	−13.3
8	5.08	6	−15.3
10	6.68	8	−16.4
12	8.28	10	−17.2

where the exponents  $\theta_n = 2\phi_n - n\phi_2$  encode the structure function scaling via  $\phi_n = \frac{1}{2}(q - \zeta_q)$ . Here,  $q = q(n)$  is determined through  $n = \frac{1}{2}(q + \zeta_q)$ , with  $\phi_n$  being the scaling exponents for moments of the VG  $\langle (\partial_x u)^n \rangle \propto \text{Re}^{\phi_n} \propto \text{Re}_\lambda^{2\phi_n}$ . This indeed yields Eq. (8) when starting from Eq. (10), with  $\phi_n = n - 1$ . Conversely, given the mapping  $n \mapsto \theta_n$ , which we find using instanton calculus, we need to invert this construction to obtain  $q \mapsto \zeta_q$ . We fix the exact relation  $\zeta_3 = 1$  [2], such that  $\phi_2 = 1$ , for this inversion to uniquely determine  $\phi_n$  from  $\theta_n$  for even integers  $n \geq 2$ .

*Results.* We show the obtained VG moments from the instanton calculations, compared to DNS and known theoretical results, in Fig. 1.  $\text{Re}_\lambda$  on the horizontal axis is found from DNS. VG moments from DNS for  $n > 8$  could not be estimated since more tail data would be required. In contrast, the instanton approximation (4) can be evaluated arbitrarily far into the PDF tails. The DNS results show a clear crossover at  $\text{Re}_\lambda \approx 1$  to the scaling (8) [34]. Without the one-loop prefactor  $C(a)$  in Eq. (4), and integrating only  $\rho(a) \approx \text{const} \times \exp(-S^I(a)/\sigma^2)$  for the numerator and denominator of Eq. (1), the bare instanton fails to capture this transition (dotted lines in Fig. 1; with  $\text{const.}$  chosen to normalize the PDF to integral 1). By including the prefactor  $C(a)$ , i.e., integrating Eq. (4) for numerator and denominator moments in Eq. (1), the change of scaling at  $\text{Re}_\lambda \approx 1$  is correctly captured (solid lines in Fig. 1). Hence, accounting for fluctuations around instantons is crucial here. Still, no clean power law scaling at  $\text{Re}_\lambda \gtrsim 1$  is visible, and the slope of the predicted  $M_n$  is too steep compared to the theoretically known result Eq. (8). In order to understand this discrepancy, we show the moment integrand  $a^n \rho(a)$  for different  $n$  in Fig. 5. This confirms that Eq. (4) becomes more accurate as  $n$  increases, but, as discussed in Ref. [44], a constant factor is missing from the PDF approximation (while the PDF tail scaling is already very well captured). This factor stems from the fact that the Gaussian approximation deviates from the true PDF, thereby producing an incorrect normalization. Motivated by this insight, we rescale the one-loop instanton PDF (4) by a constant,  $\text{Re}$ -dependent factor for  $a < 0$  to match the left tails of the respective DNS PDF (cf. Table I). Furthermore, we use DNS instead of instantons to evaluate the denominator in Eq. (1), since the second moment is not a tail quantity and cannot

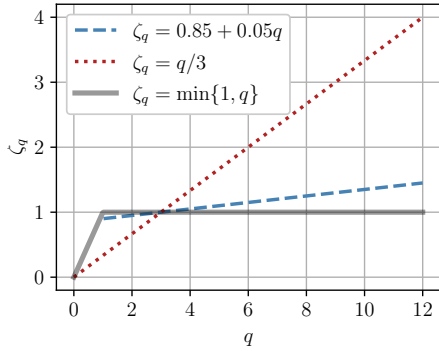


FIG. 2. Exact structure function exponents  $\zeta_q$  (grey, solid) for the Burgers Eq. (2), K41 theory prediction (red, dotted), and exponents from instantons and fusion rules (blue, dashed).

be accurately captured by the instanton approximation in its current form (cf. Fig. 5). These two changes lead to the dashed lines in Fig. 1, which display clean power law scaling and excellently match DNS data where available. Linear regression on the obtained  $(\log \text{Re}_\lambda, \log M_n)$  prediction for  $\text{Re}_\lambda > 2$  yields the scaling exponents  $\theta_n$  of the normalized VG moments listed in Table I. Remaining errors can partially be attributed to the small  $\text{Re}_\lambda$  considered here, as the DNS data shows (cf. also Fig. 4). Nevertheless, the trend is very promising. If we suppose  $\zeta_q = \alpha + \frac{1-\alpha}{3}q$  for the structure function exponents with  $\alpha$  to be determined ( $\beta$ -model), then the linear slope of  $n \mapsto \theta_n$  from Table I is consistent with  $\zeta_q \approx 0.85 + 0.05q$ . Although this prediction for the scaling exponents does not exactly reproduce the known Burgers result (10), cf. Fig. 2, it is important to emphasize that it is obtained from a fully controllable method applied directly to the evolution equations. In order to avoid reliance on low-order moments, a possible approach is to use ideas from extended self-similarity (ESS) [59, 60] and compare only high VG moments – avoiding input from DNS altogether since not even  $\text{Re}_\lambda$  as a function of  $\sigma^2$  is needed. As an example, we show  $\langle (\partial_x u)^n \rangle$  as a function of  $\langle (\partial_x u)^{n_*} \rangle$  in Fig. 3 for  $n_* = 6$ . Circles show DNS results, grey lines the theoretically expected exponent  $\frac{n-1}{n_*-1}$ , and colored lines are produced directly from Eq. (4). As expected, we see that focusing on high moments gives excellent agreement with the theory and thus demonstrates that high order structure function scaling can be predicted by our approach.

*Conclusion and Outlook.* In this Letter, we use the instanton approach together with fusion rules at the onset of turbulence to infer the scaling exponents of structure functions in fully developed Burgers turbulence. This approach offers a systematic framework that can capture the turbulent regime. Our overall strategy has been to use instanton calculus where it gives accurate results – at moderate  $\text{Re}$ , and for dissipative VG tail events – and combine it with additional input – fusion rules

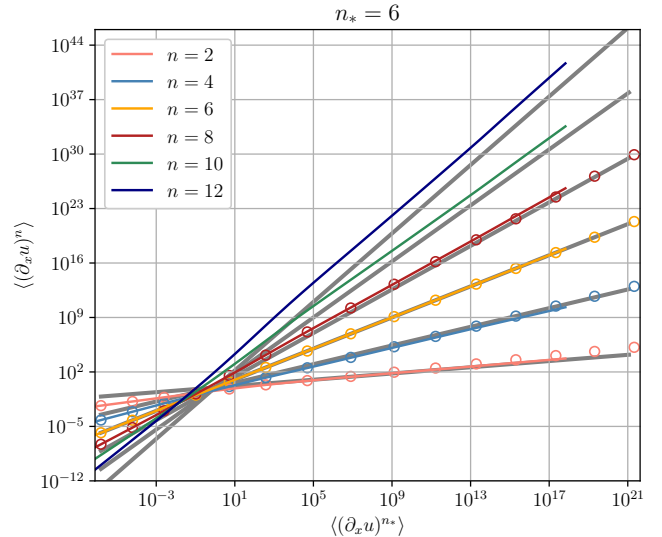


FIG. 3. ESS plot for VG moments.

– to “upscale” to the inertial range in fully developed turbulence. An important future direction is the application of this approach to the 3D NSE. While computationally more challenging, such an extension is feasible [42, 53] and might produce structure function exponents in even closer agreement with experimental and DNS data since intermittency is reduced compared to the Burgers case. A shortcoming of the method, as presented here, is the need for information from DNS for low-order quantities, which fall outside the applicability of the instanton approach (such as the second moment and normalization). To address this limitation, we have suggested an ESS-like approach. Several other strategies are under consideration for future work. A natural extension of the present approach is to include not only quadratic, but also higher-order perturbations around the instanton. This approach would lead to evolution equations for higher-order ( $d \geq 3$ ) tensors compared to the Riccati equation of Ref. [51] of dimensionality  $N^d$ , where  $N$  denotes the number of degrees of freedom (mesh points or Fourier modes), thus requiring additional low rank techniques [61, 62]. An even more challenging direction is to study the stochastic equation around the instanton [63] using methods from functional renormalization [21]. A first step in this direction has been presented in Refs. [64, 65]. Arguably the central challenge is to identify which fluctuations provide the leading contributions to the path integral, potentially those associated with slightly broken zero modes. Establishing this understanding may represent a decisive step toward a theory of turbulence.

*Acknowledgments.* RG acknowledges support from the German Research Foundation DFG within the Collaborative Research Center SFB1491.



\* [timo.schorlepp@nyu.edu](mailto:timo.schorlepp@nyu.edu)

† [grauer@tp1.rub.de](mailto:grauer@tp1.rub.de)

- [1] K. R. Sreenivasan and J. Schumacher, *Annu. Rev. Condens. Matter Phys.* **16**, 121 (2025).
- [2] U. Frisch, *Turbulence: the legacy of AN Kolmogorov* (Cambridge university press, 1995).
- [3] C. Meneveau and K. R. Sreenivasan, *J. Fluid Mech.* **224**, 429–484 (1991).
- [4] Z.-S. She and E. Leveque, *Phys. Rev. Lett.* **72**, 336 (1994).
- [5] B. Dubrulle, *Phys. Rev. Lett.* **73**, 959 (1994).
- [6] R. Grauer, J. Krug, and C. Marliani, *Phys. Lett. A* **195**, 335 (1994).
- [7] V. Yakhot, *Phys. Rev. E* **63**, 026307 (2001).
- [8] V. Yakhot, *Phys. D: Nonlinear Phenom.* **215**, 166 (2006).
- [9] C. Eling and Y. Oz, *J. High Energy Phys.* **2015** (9), 150.
- [10] G. B. Apolinário, L. Moriconi, R. M. Pereira, and V. J. Valadão, *Phys. Rev. E* **102**, 041102 (2020).
- [11] J. Duchon and R. Robert, *Nonlinearity* **13**, 249 (2000).
- [12] R. H. Kraichnan, *J. Fluid Mech.* **5**, 497–543 (1959).
- [13] H. Wyld, *Annals of Physics* **14**, 143 (1961).
- [14] V. Yakhot and S. A. Orszag, *Phys. Rev. Lett.* **57**, 1722 (1986).
- [15] N. V. Antonov, S. V. Borisenok, and V. I. Girina, *Theor. Math. Phys.* **106**, 75 (1996).
- [16] V. L’vov and I. Procaccia, *Phys. Rev. Lett.* **76**, 2898 (1996).
- [17] R. Benzi, L. Biferale, and F. Toschi, *Phys. Rev. Lett.* **80**, 3244 (1998).
- [18] J. Schumacher, K. R. Sreenivasan, and V. Yakhot, *New J. Phys.* **9**, 89 (2007).
- [19] J. P. Bouchaud, M. Mézard, and G. Parisi, *Phys. Rev. E* **52**, 3656 (1995).
- [20] S. Mathey, T. Gasenzer, and J. M. Pawłowski, *Phys. Rev. A* **92**, 023635 (2015).
- [21] L. Canet, *J. Fluid Mech.* **950**, P1 (2022).
- [22] C. Fontaine, M. Tarpin, F. Bouchet, and L. Canet, *SciPost Phys.* **15**, 212 (2023).
- [23] V. Gurarie and A. Migdal, *Phys. Rev. E* **54**, 4908 (1996).
- [24] G. Falkovich, I. Kolokolov, V. Lebedev, and A. Migdal, *Phys. Rev. E* **54**, 4896 (1996).
- [25] E. Balkovsky, G. Falkovich, I. Kolokolov, and V. Lebedev, *Phys. Rev. Lett.* **78**, 1452 (1997).
- [26] G. Falkovich and V. Lebedev, *Phys. Rev. E* **83**, 045301 (2011).
- [27] T. Grafke, R. Grauer, and T. Schäfer, *J. Phys. A: Math. Theor.* **48**, 333001 (2015).
- [28] G. B. Apolinário, L. Moriconi, and R. M. Pereira, *Phys. Rev. E* **99**, 033104 (2019).
- [29] A. Fuchs, C. Herbert, J. Rolland, M. Wächter, F. Bouchet, and J. Peinke, *Phys. Rev. Lett.* **129**, 034502 (2022).
- [30] S. Bureković, T. Schäfer, and R. Grauer, *Phys. Rev. Lett.* **133**, 077202 (2024).
- [31] A. A. Migdal, *Int. J. Mod. Phys. A* **09**, 1197 (1994).
- [32] A. Migdal, *Universal Area Law in Turbulence* (2019), [arXiv:1903.08613 \[hep-th\]](https://arxiv.org/abs/1903.08613).
- [33] K. P. Iyer, S. S. Bharadwaj, and K. R. Sreenivasan, *Proc. Natl. Acad. Sci. U.S.A.* **118**, e2114679118 (2021).
- [34] J. Friedrich, G. Margazoglou, L. Biferale, and R. Grauer, *Phys. Rev. E* **98**, 023104 (2018).
- [35] S. Khurshid, D. A. Donzis, and K. R. Sreenivasan, *Phys. Rev. E* **107**, 045102 (2023).
- [36] V. Yakhot and D. Donzis, *Phys. Rev. Lett.* **119**, 044501 (2017).
- [37] T. Gotoh and J. Yang, *Phil. Trans. R. Soc. A* **380**, 20210097 (2022).
- [38] M. Carbone and M. Wilczek, *J. Fluid Mech.* **986**, A25 (2024).
- [39] J. M. Burgers, *Adv. Appl. Mech.* **1**, 171 (1948).
- [40] U. Frisch and J. Bec, in *New trends in turbulence. Turbulence: nouveaux aspects: 31 July–1 September 2000* (Springer, 2002) pp. 341–383.
- [41] J. Bec and K. Khanin, *Phys. Rep.* **447**, 1 (2007).
- [42] T. Schorlepp, T. Grafke, S. May, and R. Grauer, *Phil. Trans. R. Soc. A* **380**, 20210051 (2022).
- [43] T. Schorlepp, T. Grafke, and R. Grauer, *J. Stat. Phys.* **190**, 50 (2023).
- [44] T. Schorlepp, K. Kormann, J. Lübke, T. Schäfer, and R. Grauer, *Phys. Rev. E* **112**, 055108 (2025).
- [45] P. C. Martin, E. Siggia, and H. Rose, *Phys. Rev. A* **8**, 423 (1973).
- [46] H.-K. Janssen, *Z. Phys. B: Condens. Matter* **23**, 377 (1976).
- [47] C. de Dominicis, *J. Phys. Colloq* **37**, 247 (1976).
- [48] A. I. Chernykh and M. G. Stepanov, *Phys. Rev. E* **64**, 026306 (2001).
- [49] T. Grafke, R. Grauer, T. Schäfer, and E. Vanden-Eijnden, *Europhys. Lett.* **109**, 34003 (2015).
- [50] E. Simonnet, *J. Comput. Phys.* **491**, 112349 (2023).
- [51] T. Schorlepp, T. Grafke, and R. Grauer, *J. Phys. A: Math. Theor.* **54**, 235003 (2021).
- [52] F. Bouchet and J. Reygner, *J. Stat. Phys.* **189**, 1 (2022).
- [53] T. Schorlepp, S. Tong, T. Grafke, and G. Stadler, *Stat. Comput.* **33**, 137 (2023).
- [54] T. Grafke, T. Schäfer, and E. Vanden-Eijnden, *Commun. Pure Appl. Math.* **77**, 2268 (2024).
- [55] T. Schorlepp and T. Grafke, *Scalability of the second-order reliability method for stochastic differential equations with multiplicative noise* (2025), [arXiv:2502.20114 \[stat.CO\]](https://arxiv.org/abs/2502.20114).
- [56] L. Onsager and S. Machlup, *Phys. Rev.* **91**, 1505 (1953).
- [57] S. Machlup and L. Onsager, *Phys. Rev.* **91**, 1512 (1953).
- [58] R. B. Lehoucq, D. C. Sorensen, and C. Yang, *ARPACK users’ guide: solution of large-scale eigenvalue problems with implicitly restarted Arnoldi methods* (SIAM, 1998).
- [59] R. Benzi, S. Ciliberto, R. Tripiccone, C. Baudet, F. Massaioli, and S. Succi, *Phys. Rev. E* **48**, R29 (1993).
- [60] R. Benzi, S. Ciliberto, C. Baudet, G. R. Chavarria, and R. Tripiccone, *Europhys. Lett.* **24**, 275 (1993).
- [61] T. Breiten, S. Dolgov, and M. Stoll, *Numer. Algebra Control Optim.* **11**, 407 (2021).
- [62] A. Rodgers and D. Venturi, *Phys. Rev. E* **110**, 015310 (2024).
- [63] L. Ebener, G. Margazoglou, J. Friedrich, L. Biferale, and R. Grauer, *Chaos* **29**, 063102 (2019).
- [64] F. Ihssen and J. M. Pawłowski, *Ann. Physics* **481**, 170177 (2025).
- [65] A. Bonanno, F. Ihssen, and J. M. Pawłowski, *Tunneling with physics-informed RG flows in the anharmonic oscillator* (2025), [arXiv:2504.03437 \[hep-th\]](https://arxiv.org/abs/2504.03437).

TABLE II. Noise variances  $\sigma^2$  and Taylor-Reynolds numbers  $\text{Re}_\lambda$  in DNS of Eq. (2), and normalization of one-loop PDFs (4) before and after rescaling the left tail by the listed constant to match DNS PDF tails.

$\sigma^2$	$\text{Re}_\lambda$	color in Fig. 5	$\int_{-\infty}^{\infty} \text{Eq. (4)} da$	left tail rescale	$\int_{-\infty}^{\infty} \text{Eq. (4)} da$ after rescaling
0.010	0.04	•	0.999935	1	0.999935
0.034	0.07	•	0.999822	1	0.999822
0.117	0.13	•	0.999473	1	0.999473
0.398	0.23	•	0.998309	1	0.998309
1.359	0.42	•	0.994445	1	0.994445
4.642	0.76	•	0.982510	1	0.982510
15.849	1.31	•	0.952587	1.1	0.992669
54.117	2.07	•	0.901730	1.2	0.965919
184.785	3.08	•	0.850983	1.5	0.964793
630.957	4.35	•	0.832163	2	0.978337
2154.435	5.90	•	0.864512	3	1.040367
7356.423	7.86	•	0.954953	5	1.158280
25118.864	10.17	•	1.109413	11	1.396104
85769.590	13.06	•	1.346033	24	1.711882
292864.456	16.48	•	1.731763	65	2.290340

## Appendix

This section contains additional figures and tables, referenced in the main text. Fig. 4 shows the dependence of  $\text{Re}_\lambda$  on the forcing strength  $\sigma^2$  in DNS, Fig. 5 shows the integrands  $a^n \rho(a)$  for the VG moments (1), and Table II lists further parameters and rescaling constants to match DNS PDF tails with the instanton approximation (4).

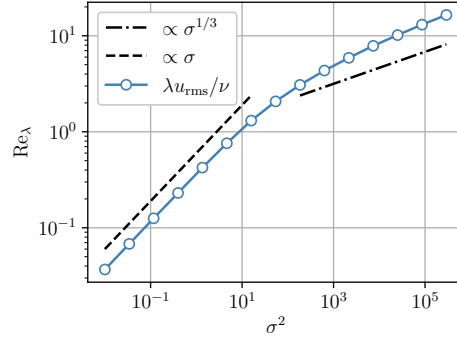


FIG. 4. Taylor-Reynolds number  $\text{Re}_\lambda = \lambda u_{\text{rms}}/\nu$  as a function of the forcing strength  $\sigma^2$  from DNS of (2).

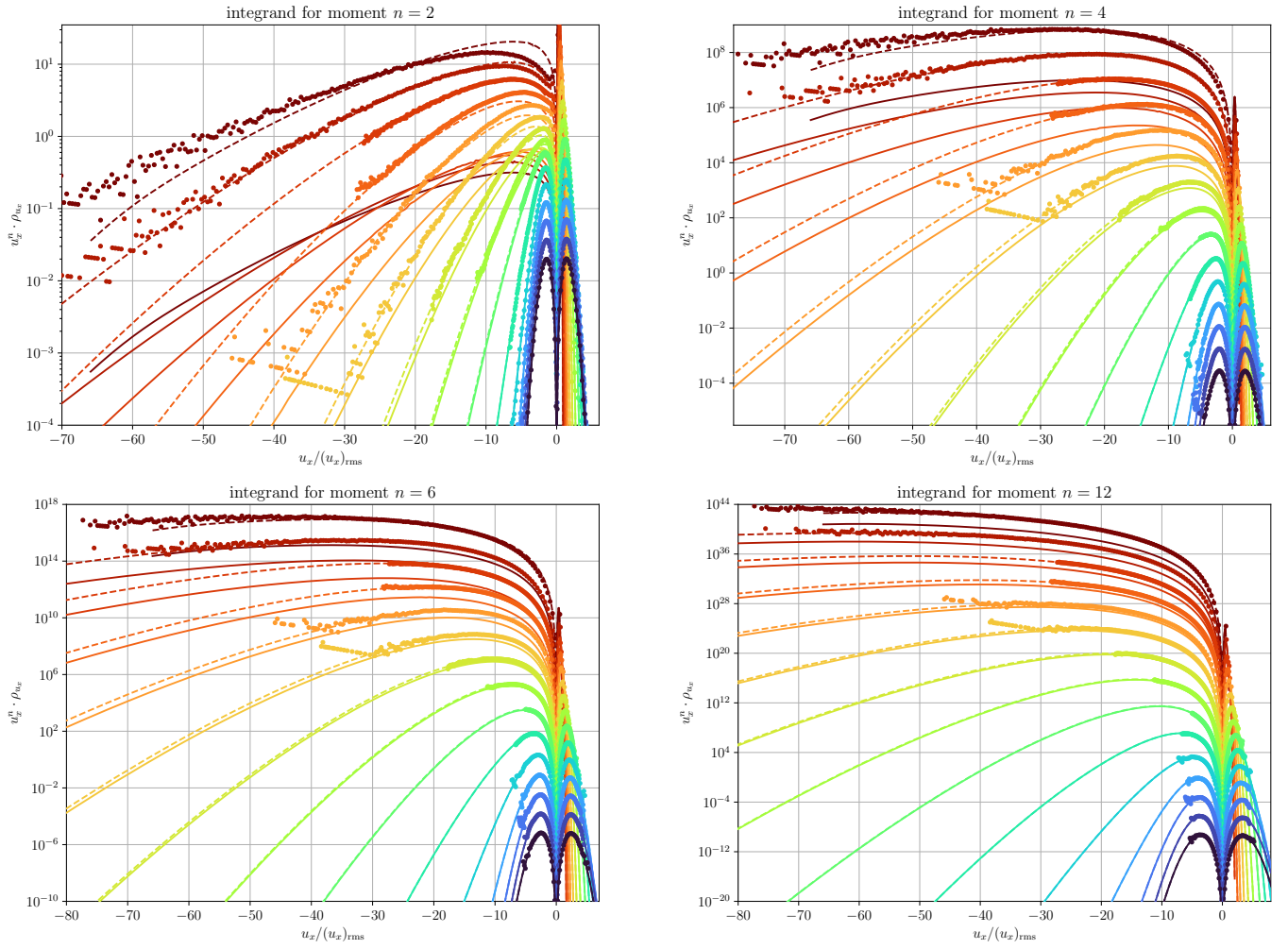


FIG. 5. Moment integrands  $a^n \rho(a)$  of the VG PDF. Dots show DNS data, solid lines show Eq. (4), and dashed lines are the same curves multiplied by a constant (cf. Table II) for  $a < 0$  to match DNS PDF tails. See Table II for noise variances  $\sigma^2$  and Taylor–Reynolds numbers  $\text{Re}_\lambda$  that different colors correspond to. Note that bin ranges for DNS PDFs were set automatically and do not capture the full range of available data for some  $\text{Re}_\lambda$ . This does not affect other results, as DNS VG moments were computed directly from field data without binning.